Int J Adv Manuf Technol (2011) 55:275–283
DOI 10.1007/s00170-010-3024-5

ORIGINAL ARTICLE

Measurement and compensation for volumetric positioning errors of CNC machine tools considering thermal effect

Hongtao Zhang · Jianguo Yang · Yi Zhang · Jinhua Shen · Charles Wang

Received: 18 June 2010 / Accepted: 3 November 2010 / Published online: 25 November 2010

Abstract The measurement and compensation of volumetric positioning errors can be used to significantly improve the accuracy of machine tools. In this paper, a sequential step diagonal measurement is introduced to measure nine volumetric positioning errors in a short time. Measurements under various thermal conditions are preformed to understand the relationship between the volumetric positioning errors and the machine temperature field and variations. A radial basis function neural network is used to predict the volumetric positioning errors at all positions based on the temperature distribution of the machine. Compensation experiment is carried out to validate the performance of the measurement and the prediction method. The experimental results show that the volumetric accuracy of the machine tool is significantly improved by the error compensation.

Keywords Machine tools · Volumetric positioning errors · Diagonal measurement · Neural network · Error compensation

H. Zhang · J. Yang · Y. Zhang (✉) · J. Shen
School of Mechanical Engineering,
Shanghai Jiao Tong University,
Shanghai 200030, People's Republic of China
e-mail: zhangyitop@gmail.com

H. Zhang
e-mail: zhanght@sjtu.edu.cn

C. Wang
Optodyne, Inc.,
Compton, CA 90220, USA
e-mail: jgyang@sjtu.edu.cn

1 Introduction

Computer numerical controlled (CNC) machine tools with high volumetric positioning accuracy are required, because of the growing demand of precision components in manufacturing. In recent years, many researches have been carried out on the compensation for volumetric positioning errors of machine tools [1–3]. To implement the error compensation scheme, it is necessary to measure the machining errors first. A laser interferometer system is most widely used for machine tool calibration even though many other measurement techniques are also used, such as the double ball bar [4, 5] or the cross-grid encoder method [6].

There are two ways to obtain the volumetric positioning errors, direct error measurement, and indirect error measurement. For direct error measurement, only one component of volumetric positioning errors can be measured at one time. This makes the measurement a tedious and time-consuming task. For this reason, many measurement methods have been proposed to improve the measurement efficiency. With these methods, the volumetric error components are identified with the combination of the measurement results and the volumetric error model derived with the rigid body kinematics [2, 7]. Zhang et al. [8] developed a displacement method to obtain the error components by measuring the errors along 22 lines. Some lines were constrained along specific paths, which made the method difficult to implement. Chen et al. [9] proposed an auto-alignment laser interferometer system which can quickly measure the 21 error components along 22 lines. Chen et al. [10] further improved Zhang's approach by measuring the positioning errors along only 15 lines.

Kiridena et al. [11] mapping the effects of positioning errors on the volumetric accuracy of five-axis CNC machine tools. Wang [12] and Shen et al. [13] proposed a laser vector or sequential step diagonal measurement technique to determination the volumetric positioning errors by modifying the body diagonal displacement test method in ISO230-6 [14]. By measuring the four body diagonal displacement, nine positioning errors can be determined. The results can be used for the compensation of volumetric positioning errors.

These laser measurement methods improve the efficiency on the determining of machine accuracy, but in most of these measurement and compensation research works, few of them have considered the thermal effect. Some of them assumed that the volumetric positioning errors do not change with temperature and can be compensated by the measurement values. But in a real machine shop environment and under various spindle loads, the machine thermal expansion may cause large 3D volumetric positioning errors [15–17]. To further improve the machine positioning accuracy, the relationship between 3D volumetric positioning errors and the thermal fields of the machine tools should be understood.

In this paper, the basic principle of sequential step diagonal measurement to calibrate nine volumetric positioning errors in a short time is introduced. To understand the relationship between the volumetric positioning errors and the temperature field variation, measurements under various thermal conditions are preformed. To compensate the volumetric positioning errors with thermal effect, a radial basis function (RBF) neural network is used to predict the volumetric positioning errors at all positions with temperature distribution of the machine. Compensation experiment is carried out to validate the performance of the measurement scheme and the prediction method.

2 Analysis of volumetric positioning error

Considering a machine motion from initial point A to the target point B, if there are no machine volumetric errors, the ideal target point should be B_i with the motion of x_i, y_i, z_i in the ideal or nominal coordinate system (X_i, Y_i, Z_i), as shown in Fig. 1. However, the real point would be the B_r because of the existence of the machine volumetric errors which make the real motion coordinate system different with the ideal coordinate system. The errors Δx, Δy, Δz between B_i and B_r in nominal coordinate system are the volumetric error in the X, Y, Z.

In a rigid body motion, there are six different errors of a single axis motion, they are linear displacement error, straightness errors—horizontal and vertical and angular errors—pitch, yaw, and roll. Thus for a three-axis machine, there are six errors per axis or a total of 18 errors plus 3 squareness errors. These 21 rigid body errors can be expressed as the followings: linear displacement errors $\delta_x(x)$, $\delta_y(y)$, $\delta_z(z)$; straightness errors $\delta_y(x)$, $\delta_z(x)$, $\delta_x(y)$, $\delta_z(y)$, $\delta_x(z)$, $\delta_y(z)$; angular errors $\varepsilon_x(x)$, $\varepsilon_y(x)$, $\varepsilon_z(x)$, $\varepsilon_x(y)$, $\varepsilon_y(y)$, $\varepsilon_z(y)$, $\varepsilon_x(z)$, $\varepsilon_y(z)$, $\varepsilon_z(z)$; and squareness errors ε_{xy}, ε_{yz}, ε_{xz}.

A volumetric error model is machine dependent and can be derived from the kinematic chain of the machine structure [12]. For a vertical machine with the workpiece fixed on X and Y sliders, as shown in Fig. 2, the volumetric error model can be expressed as:

$$\begin{aligned}\Delta x &= \delta_x(x) + \delta_x(y) + \delta_x(z) + \varepsilon_y(x)\cdot z + \varepsilon_y(y)\cdot z + \varepsilon_{xz}\cdot z + \varepsilon_{xy}\cdot y\\ \Delta y &= \delta_y(x) + \delta_y(y) + \delta_y(z) + \varepsilon_x(x)\cdot z + \varepsilon_x(y)\cdot z - \varepsilon_z(x)\cdot x + \varepsilon_{yz}\cdot z\\ \Delta z &= \delta_z(x) + \delta_z(y) + \delta_z(z) - \varepsilon_x(y)\cdot y - \varepsilon_y(y)\cdot x\end{aligned} \tag{1}$$

For most machine tools, the pitch, yaw, and roll angular errors are related to the straightness errors. The effect of angular errors on the positioning accuracy is the angular error times the Abbe offset. In many cases, the straightness errors measurement already include the errors caused by the angular errors times an Abbe offset. And it is very difficult for CNC to compensate the angular errors separately. Thus to simplify the compensation process, the 3D positioning errors in each axis directions can be expressed as:

$$\begin{aligned}\Delta x &= E_x(x) + E_x(y) + E_x(z)\\ \Delta y &= E_y(x) + E_y(y) + E_y(z)\\ \Delta z &= E_z(x) + E_z(y) + E_z(z)\end{aligned} \tag{2}$$

where $E_x(x)$, $E_y(y)$, $E_z(z)$ have the same value as the linear displacement errors $\delta_x(x)$, $\delta_y(y)$ and $\delta_z(y)$, and $E_x(y)$, $E_x(z)$, $E_y(x)$, $E_y(z)$, $E_z(x)$ and $E_z(y)$ are the new defined straightness errors and they are errors combined with straightness errors, angular errors and squareness errors that can be obtained by comparing with Eq. 1.

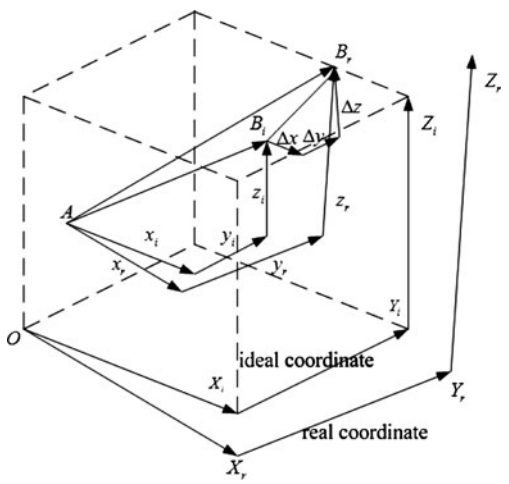

Fig. 1 Volumetric positioning errors

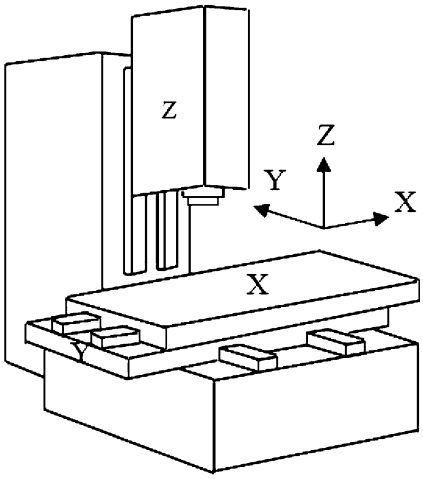

Fig. 2 Schematic for a vertical machine tool

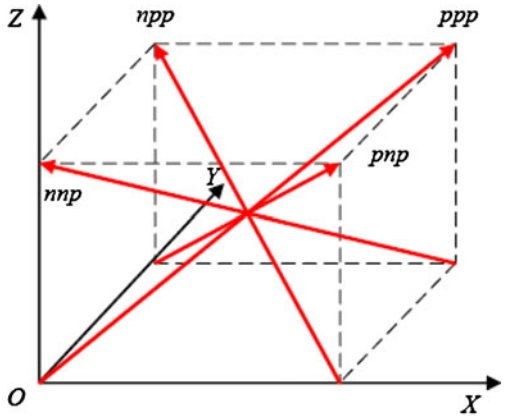

Fig. 4 Four body diagonals of the machine tool working volume

3 Sequential step diagonal measurement method

The body diagonal displacement test defined in the ASME B5.54 [18] or ISO 230-6 standard is a good and quick way to check the volumetric errors. Although it has been proved to be useful and successful, it is not clear what is the relationship between the body diagonal displacement errors and the 3D positioning errors because of the lack of enough data to identify these errors.

Compared with the conventional diagonal measurement, the data in the sequential step diagonal measurement method are collected after each axis moved an increment, while the data are collected only along the diagonal direction in the conventional diagonal measurement. As is shown in the Fig. 3, P_0 and P_1 are two measurement points respectively along the diagonal. With the conventional diagonal measurement method, first, acquire the diagonal displacement R_{P_0} of point P_0, and then move the measurement point to the P_1 by moving the *X*-, *Y*-, and *Z*-axis simultaneously, the data collected is the diagonal displacement R_{P_1}. The difference of R_{P_0} and R_{P_1} is the diagonal error *dR*. With the sequential step diagonal measurement method, first, collect the diagonal displacement R_{P_0} of point P_0, and then move D_x along the *X*-axis direction to the middle measurement point M_1 and acquire the diagonal displacement R_{M_1}, and next move D_y along the *Y*-axis direction to the second middle measurement point M_2 and also acquire the diagonal displacement R_{M_2}, finally move D_z along the *Z*-axis direction to the point P_1 and also acquire the diagonal displacement R_{P_1}. As there are four displacement values, three sets of diagonal errors can be calculated with the differences of the values one and another, which means three times more data are obtained than in the conventional diagonal measurement.

For a machine working volume, there are four body diagonals directions shown in Fig. 4. Here, *p* means positive direction while *n* means negative direction and the sequence of the three letters is ordered by *X*-, *Y*-, and *Z*-axis. Thus, 12 sets of measurement results can be identified if these four diagonals are measured; the same variable number in Eq. 2 given in the above section. With the analysis, the relationship between the variables or the nine

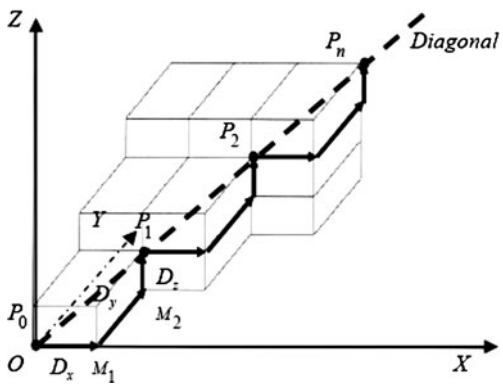

Fig. 3 Measurement path for sequential step body diagonal method

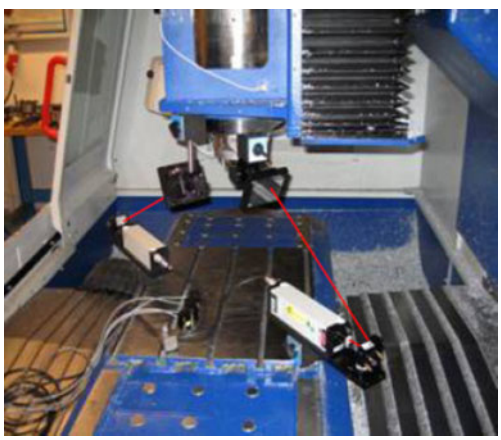

Fig. 5 Setup for the calibration laser system

Table 1 Number and locations for temperature sensors

Sensors Number	Sensors location	Sensors Number	Sensors location
1	Spindle top	7	*Y*-axis left front
2	Spindle house bottom	8	*Y*-axis left back
3	Spindle house back top	9	Basement frame top
4	*X*-axis middle front	10	Column frame top
5	*X*-axis right front	11	Column frame bottom
6	*X*-axis right back	12	Ambient temperature

new defined positioning errors and the diagonal displacement errors can be expressed as:

$$
\begin{aligned}
E_x(x) &= \left[dR(x)_{ppp} - dR(x)_{npp}\right]\frac{R}{2X}\\
E_y(x) &= \left[dR(x)_{ppp} - dR(x)_{pnp}\right]\frac{R}{2Y}\\
E_z(x) &= \left[dR(x)_{ppp} - dR(x)_{ppn}\right]\frac{R}{2Z}\\
E_x(y) &= \left[dR(y)_{ppp} - dR(y)_{npp}\right]\frac{R}{2X}\\
E_y(y) &= \left[dR(y)_{ppp} - dR(y)_{pnp}\right]\frac{R}{2Y}\\
E_z(y) &= \left[dR(y)_{ppp} - dR(y)_{ppn}\right]\frac{R}{2Z}\\
E_x(z) &= \left[dR(z)_{ppp} - dR(z)_{npp}\right]\frac{R}{2X}\\
E_y(z) &= \left[dR(z)_{ppp} - dR(z)_{pnp}\right]\frac{R}{2Y}\\
E_z(z) &= \left[dR(z)_{ppp} - dR(z)_{ppn}\right]\frac{R}{2Z}
\end{aligned}
\tag{3}
$$

where $dR(x)_{ppp}$ is the diagonal error along body diagonal *ppp* for the *X*-axis motion, and similarly for the others.

4 Measurement of volumetric positioning error

4.1 Measurement setup

The measurements were performed on a vertical machining center [19]. The machine configuration is shown in Fig. 2. The machine is equipped with linear motor drives, a cross bed with two driven axes *X*, *Y* and a vertically oriented spindle (*Z*-axis) form the structure of the machine. The measurements were performed on the machining center over a working volume of *X*=500 mm, *Y*=400 mm, and *Z*=320 mm. All measurements were performed using Optodyne laser system and there were four setups, one on each of the four body diagonal directions. To reduce the alignment time, two laser systems were aligned in the directions *ppp* and nnp as shown in Fig. 5.

In addition, 12 thermocouple temperature sensors were placed at different locations within the machine frame to measure the thermal variation of the machine tool. Table 1 gives the number of temperature sensors and their locations. As the temperature of the machine changes slowly in a normal condition, some operations were done to warm the machine warm. The duty cycle consists of a continuous spindle ran at maximal speed at 15,000 rpm and *X*-, *Y*-, and *Z*-axes motion at maximum stroke in the *ppp* diagonal direction at 50% maximum rapid feed rate. The 12 temperature sensors readings were recorded at 2-min interval starting before the measurement and ending after the measurement during the day, shown in Fig. 6.

4.2 Measurement results

During a measurement day, measurement was performed six times and then six sets of positioning error data are obtained.

For *X*-axis, the linear displacement errors $E_x(x)$, vertical straightness errors $E_y(x)$, and horizontal straightness errors $E_z(x)$ are plotted in Fig. 7a–c, respectively. For the linear

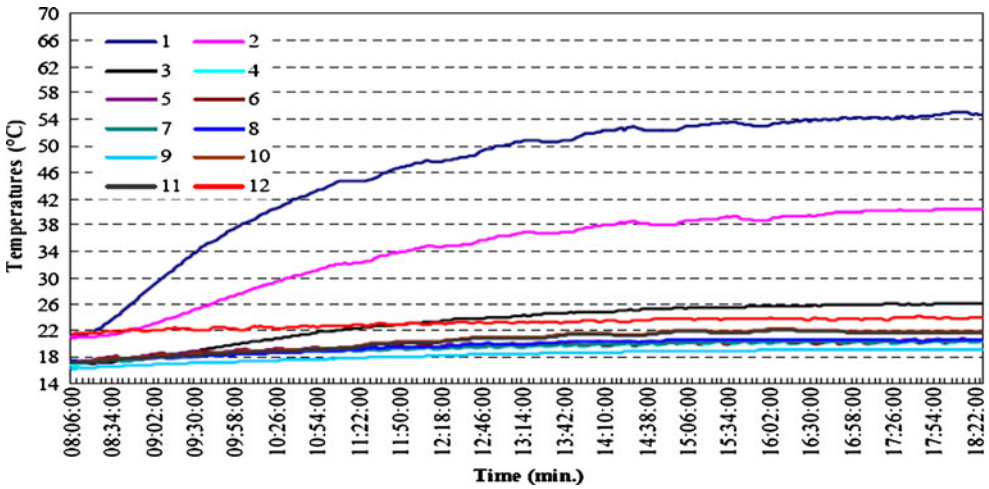

Fig. 6 Plot of the machine temperature

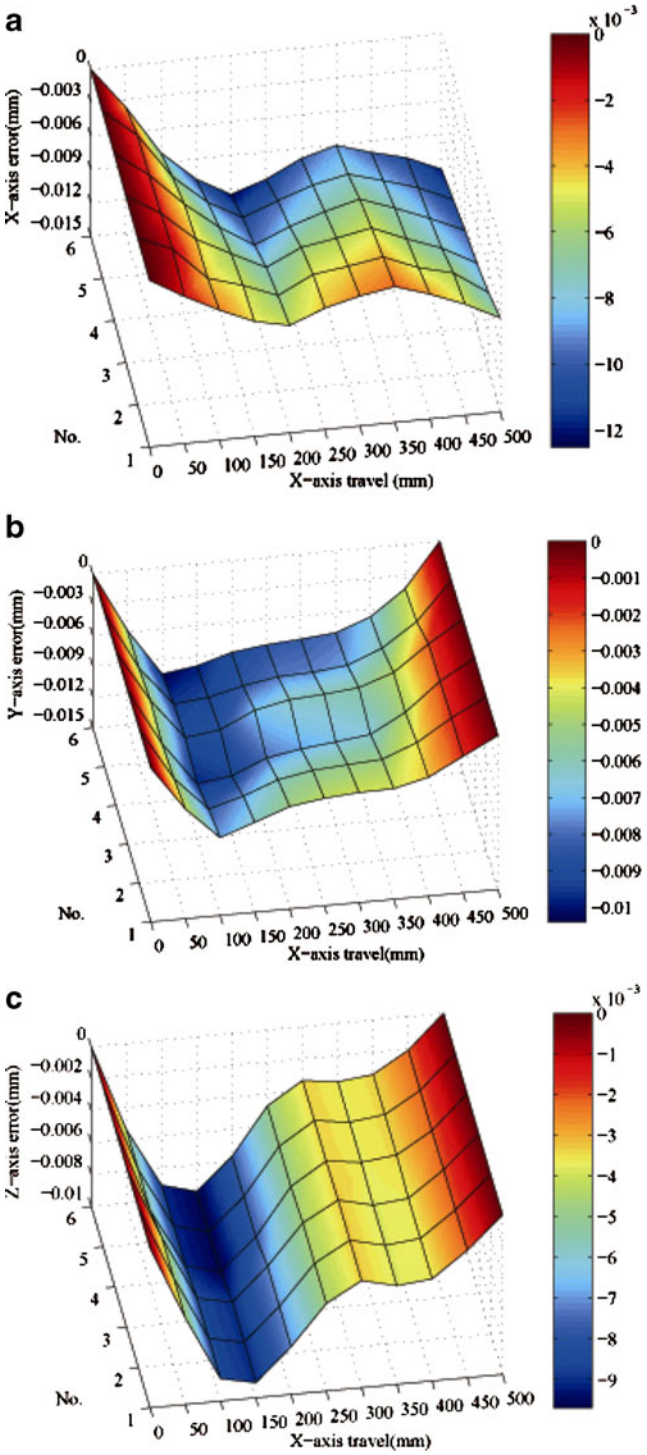

Fig. 7 *X*-axis positioning errors under different thermal condition; **a** $E_x(x)$, **b** $E_y(x)$, **c** $E_z(x)$

displacement errors $E_x(x)$, the maximal error increased from 6.5 to 12 μm at X=500 mm with 3 μm variation due to the thermal effect; for $E_y(x)$, the maximal error increased from 6.5 to 12 μm at X=100 mm with 3 μm variation; for $E_z(x)$, the maximal error increased from 9 to 10 μm at X=150 mm with only 1-μm variation. For the *X*-axis positioning errors, the change of straightness errors were relatively small over the temperature range compared with the linear displacement errors.

For *Y*-axis, as shown in Fig. 8a–c, the maximal error of linear displacement errors $E_y(y)$, increased from 4 to 8.5 μm

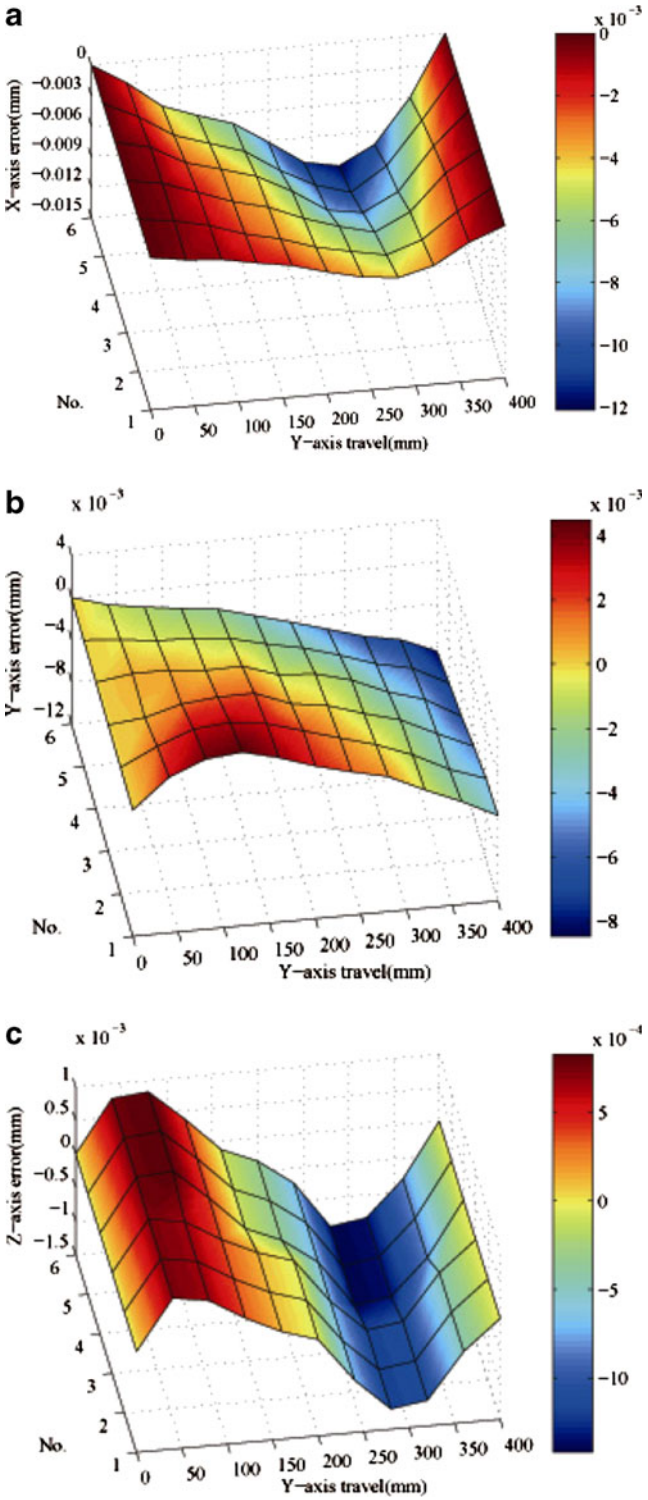

Fig. 8 *Y*-axis positioning errors under different thermal condition; **a** $E_x(y)$, **b** $E_y(y)$, **c** $E_z(y)$

at Y=400 mm with 4.5 μm variation due to the thermal effect; for $E_x(y)$, the maximal error increased from 4 to 12 μm at Y=280 mm with 8 μm variation; for $E_z(y)$, the maximal error increased from 12 to 14 μm at Y=280 mm with only 2 μm variation. For the Y-axis positioning errors, the change of linear displacement errors $E_y(y)$ and horizontal straightness errors $E_z(y)$ were similar to the X-axis. However, the change of vertical straightness errors $E_x(y)$ were larger than that of the Y-axis linear displacement errors which are quite different.

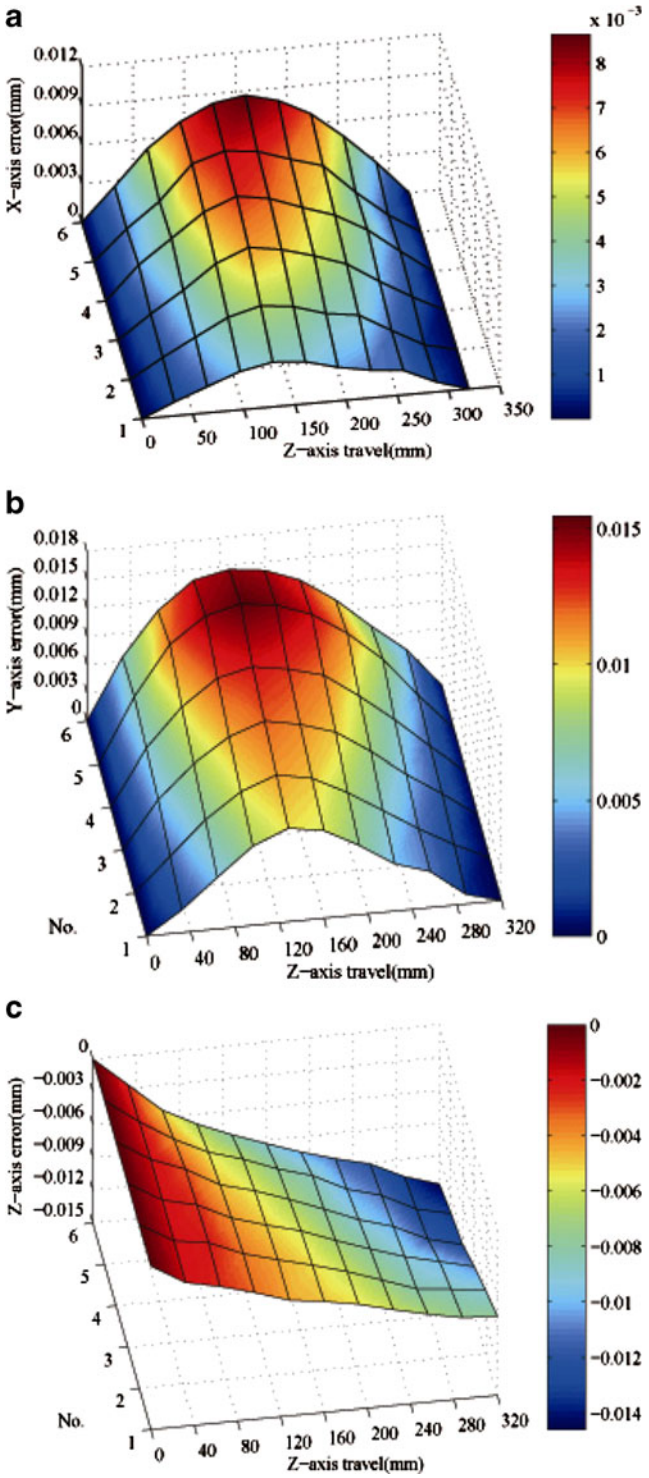

Fig. 9 Z-axis positioning errors under different thermal condition, **a** $E_x(z)$, **b** $E_y(z)$, **c** $E_z(z)$

For Z-axis, as shown in Fig. 9a–c, the maximal error of linear displacement errors $E_z(z)$, increased from 7.8 to 14.6 μm at Z=320 mm with 6.8 μm variation due to the thermal effect; for $E_x(z)$, the maximal error increased from 3.5 to 8.6 μm at between 128 and 160 mm with 8.6 μm variation; for $E_y(z)$, the maximal error increased from 10 to 14.5 μm at X=280 mm with 4.5 μm variation. For the Z-axis positioning errors, the changes of linear displacement and straightness errors are all as expected.

The measured linear displacement error data of the X-, Y-, and Z-axis were proportional to the increase of machine bed temperature or thermal growth as expected. However, vertical errors $E_x(y)$, $E_x(z)$, and $E_y(z)$ for Y- and Z-axis, the increasing of the errors were much larger. The reason for these large errors was due to the Z-axis sagging or the squareness error changes. It can found that the changes of squareness errors were 0.56, 17.11, and 7.56 arcsec in the XY, YZ, and ZX by Eq. 4.

$$\begin{aligned}\varepsilon_{yz} &= \left[dR(x)_{ppp} + dR(x)_{npp}\right]\frac{R}{2YZ}\\ \varepsilon_{zx} &= \left[dR(x)_{ppp} + dR(x)_{pnp}\right]\frac{R}{2XZ}\\ \varepsilon_{xy} &= \left[dR(x)_{ppp} + dR(x)_{ppn}\right]\frac{R}{2XY}\end{aligned} \tag{4}$$

5 Compensation of volumetric positioning errors

5.1 Prediction of volumetric positioning errors

As the volumetric positioning errors change with the temperature field of machine tool, it is necessary to consider the thermal effect when implementing the error compensation. If the volumetric positioning errors can be predicted, it will save the measurement time when the machine tool is used at different thermal condition. Here, the discussion about how to predict the volumetric positioning errors consider thermal effect is based on the Y-axis horizontal straightness error $E_x(y)$.

A simple method to predict the volumetric positioning errors is to generate a new error map at any thermal state by linear interpolation between two measured maps, shown as Eq. 5.

$$E_x(y,T_u) = E_x(y,T_m) + (E_x(y,T_n) - E_x(y,T_m))\frac{(T_u - T_m)}{(T_n - T_m)} \tag{5}$$

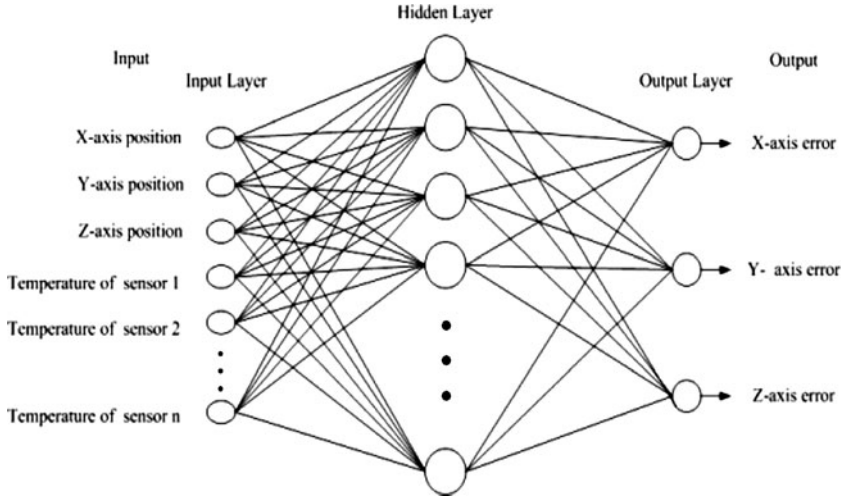

Fig. 10 Structure of RBF neural network for volumetric positioning errors prediction

where $E_x(y, T_m)$, $E_x(y, T_n)$are the measured *Y*-axis horizontal straightness error at position y under the temperature of T_m and T_n, $E_x(y, T_u)$ is a predicted error at the same position under the temperature of T_u and T_u satisfies the inequality $T_m T_u T_n$.

But the problem is that only one temperature point can be used for the error prediction and if the errors do not change in a linear way, the larger difference between temperature T_u and the temperature T_m and T_n, the less prediction accuracy will it be, which means the measured maps should be as more as possible. In addition, if $T_u > T_n$, the positioning error cannot be predicted.

For this reason, a RBF neural network is used to approximate the volumetric errors at different thermal state. The basic structure of RBF neural network for volumetric position errors prediction is shown in Fig. 10. The positions of x, y, z along *X*-, *Y*-, Z-axis of the measurement point and the temperature readings of the thermocouple temperature sensors are the input of the network, and the volumetric errors at prediction thermal state are the output of the network. The transfer function of output is linear and the

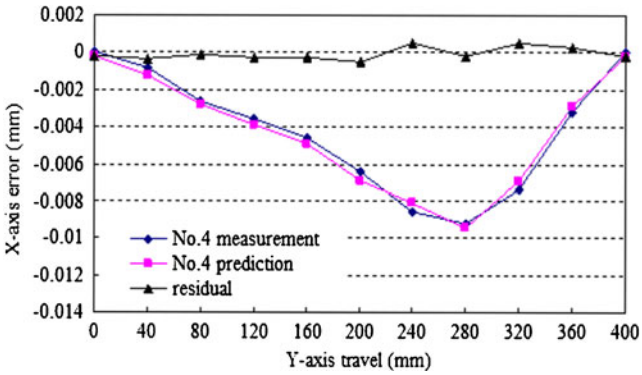

Fig. 11 Prediction results for $E_x(y)$ at run No. 4 with the rest five sets of measurement

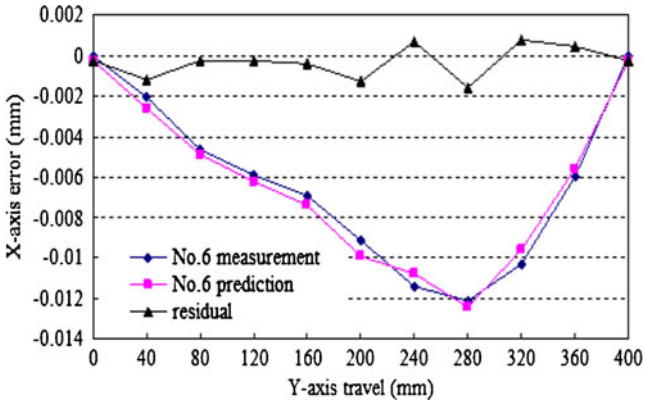

Fig. 12 Prediction results for $E_x(y)$ at run No. 6 with the rest five sets of measurement

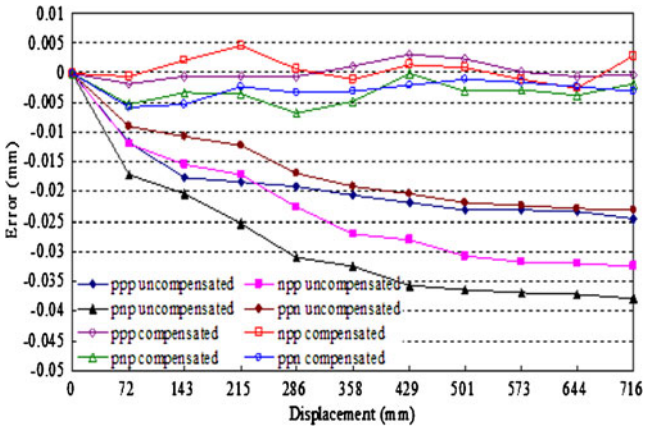

Fig. 13 Compensated and uncompensated four body diagonals displacement errors

actuation function of the hidden layer is the Gaussian function with symmetric shape given by

$$R_i(x) = \exp\left(-\frac{\|x-c_i\|^2}{2\sigma_i^2}\right) \quad , \quad i = 1, 2, 3 \cdots \tag{6}$$

where x, c_i and σ_i are the input vector, center, and width of the Gaussian, respectively,$\|\bullet\|$ denotes the Euclidean norm.

After training the network with the measured volumetric positioning errors and the temperate of the machine tool, the new volumetric positioning errors can be determined by this model. Here, the prediction results for *Y*-axis horizontal straightness error $E_x(y)$ are given. Figure 11 shows the prediction results of the No. 4 set data for $E_x(y)$ after training the rest five sets of measurement data by the RBF neural network modeling (there are six sets of data being used in the RBF neural network modeling) and is compared with the measured values. The residual of the model is within the range of −1.5 and 1 μm. Figure 12 shows the prediction results of the No. 6 set data for $E_x(y)$ and is compared with the measured values. The residual of the model is within the range of −2 and 1 μm. So it can be seen that the RBF neural network can predict the volumetric positioning error well.

5.2 Compensation of volumetric positioning errors

To evaluate the measurement method and prediction effect of volumetric positioning errors, a compensation experiment was performed. The volumetric positioning errors were predicted by the RBF neural network with the temperate and *X*-, *Y*-, *Z*-axis positions, and they were used to generate the compensation file for the machine controller. The errors along the four diagonals *ppp*, *npp*, *pnp*, *ppn* were measured with the convention diagonal measurement to verify the compensation effects.

Figure 13 shows the results of compensated and uncompensated positioning errors of the four diagonals. Before the volumetric positioning errors were compensated, the errors along the diagonal *pnp* was the worst with the maximal error of −38 μm, and then the *npp*, *ppp*, and *ppn* with the maximal error of −32, −25, and −23 μm, respectively. After the compensation, the error of diagonal *ppp* was reduced to a range of −2 and 3 μm, the error of diagonal *npp* was reduced to a range of −3 and 4.5 μm, the error of diagonal *pnp* was reduced to a range of −1 and −7 μm, the error of diagonal *ppn* was reduced to a range of 0 and −5.5 μm.

6 Conclusion

The sequential step diagonal measurement is proposed in this paper to calibrated nine volumetric positioning errors under various thermal conditions. The measurement results show that with the increase of the machine temperature field, the change of volumetric positioning errors is from 1 to 8.6 μm. A RBF neural network is used to predict the volumetric positioning errors with the axis positions and temperature points located on the machine, and the predicted errors are used for the volumetric error compensation. The compensation experimental results show that the four diagonal errors are reduced to a variation of 7 μm, the volumetric accuracy of the machine tool is much improved.

Acknowledgment The paper is sponsored by the Important National Science and Technology Specific Projects (No.2009ZX04014-22).

References

1. Ji-Hun J, Jin-Phil C, Sang-Jo L (2006) Machining accuracy enhancement by compensating for volumetric errors of a machine tool and on-machine measurement. Mater Process Technol 174:56–66
2. Okafor AC, Ertekin YM (2000) Derivation of machine tool error models and compensation procedure for three axis vertical machining center using rigid body kinematic. Int J Mach Tools Manuf 40:1199–1213
3. Wang SM, Liu YL, Kang Y (2002) An efficient error compensation system for CNC multi-axis machines. Int J Mach Tools Manuf 42:1235–1245
4. Lee ES, Suh SH, Shon JW (1998) A comprehensive method for calibration of volumetric positioning accuracy of CNC machines. Int J Adv Manuf Technol 14:43–49
5. Pahk HJ, Kim YS, Moon JH (1997) A new technique for volumetric error assessment of CNC machine tools incorporating ball bar measurement and 3D volumetric error model. Int J Mach Tools Manuf 37:1583–1596
6. Ibaraki S, Kakino Y, Lee K, Ihara Y, Braasch J, Eberherr A (2001) Diagnosis and compensation of motion errors in CNC machine tools by arbitrary shape contouring error measurement. Laser metrology and machine performance V. WIT press, Southampton
7. Ahn KG, Cho DW (1999) Proposition for a volumetric error model considering backlash in machine tools. Int J Adv Manuf Technol 15:554–561
8. Zhang GX, Ouyang R, Lu B (1988) A displacement method for machine geometry calibration. Ann CIRP 37:515–518
9. Chen JS, Kou TW, Chiou SH (1999) Geometic error calibration of multi-axis machines using an auto-alignment laser interferometer. Precis Eng 23:243–252
10. Chen G, Yuan J, Ni J (2001) A displacement measurement approach for machine geometric error assessment. Int J Mach Tools Manuf 41:149–161
11. Kiridena V, Ferreira PM (1993) Mapping the effects of positioning errors on the volumetric accuracy of five-axis CNC machine tools. Int J Mach Tools Manuf 33:417–437
12. Wang C (2000) Laser vector measurement technique for the determination and compensation of volumetric positioning errors. Part I: basic theory. Review of Scientific Instruments 71 (10):3933–3937
13. Shen JH, Zhao HT, Cao HT, Yang JG, Wang C (2006) Volumetric positioning errors of CNC machine tools and laser sequential step diagonal measurement. Key Eng Mater 315 –316:98–102

14. ISO 230-6 (2002). Test code for machine tools, part 6. Determination of positioning accuracy on body and face diagonals (diagonal displacement tests). ISO.
15. Shen J.H., Yang J.G. and Wang C. (2008) Analysis on volumetric positioning error development due to thermal effect based on the diagonal measurement. Advanced design and manufacture to gain a competitive edge. Springer: London, UK. August 2008 (ISBN: 978-1-84800-240-1):293 –302.
16. Pahk HJ, Lee SW (2002) Thermal error measurement and real time compensation system for the CNC machine tools incorporating the spindle thermal error and the feed axis thermal error. Int J Adv Manuf Technol 20:487–494
17. Yan JY, Yang JG (2009) Application of synthetic grey correlation theory on thermal error compensation. Int J Adv Manuf Technol 43:1124–1132
18. ASME B5.54. (1992) Methods for performance evaluation of computer numerical controlled machining centres. ASME
19. Svoboda O. (2007) Milling machine tool's accuracy in thermally unbalanced conditions, Ph.D. Thesis, Czech Technical University in Prague, July 2007